0013-7227/02/$15.00/0
*Printed in U.S.A.*

Endocrinology 143(7):2797–2807
Copyright © 2002 by The Endocrine Society

# Prevention of Thecal Angiogenesis, Antral Follicular Growth, and Ovulation in the Primate by Treatment with Vascular Endothelial Growth Factor Trap R1R2

CHRISTINE WULFF, HELEN WILSON, STANLEY J. WIEGAND, JOHN S. RUDGE, AND HAMISH M. FRASER

*Medical Research Council (C.W., H.W., H.M.F.) Human Reproductive Sciences Unit, Edinburgh, United Kingdom EH3 9ET; Department of Obstetrics and Gynecology, University of Ulm (C.W.), 89075 Ulm, Germany; and Regeneron Pharmaceuticals, Inc. (S.J.W., J.S.R.), Tarrytown, New York 10591*

Downloaded from https://academic.oup.com/endo/article/143/7/2797/2989719 by Associated Press user on 06 January 2023

**This study was designed to investigate the effects of inhibition of thecal angiogenesis on follicular development in the marmoset monkey (*Callithrix jacchus*). To inhibit vascular endothelial growth factor (VEGF), a soluble combined truncated form of the fms-like tyrosine kinase (Flt) and kinase insert domain-containing receptor (KDR) receptor fused to IgG (VEGF Trap R1R2) was administered for 10 d during the follicular phase of the cycle. Changes in angiogenesis and follicular cell proliferation were quantified using immunocytochemistry for bromodeoxyuridine to obtain a proliferation index, CD31 to visualize endothelial cell area, and dual staining to distinguish thecal endothelial cell proliferation. The effects of the treatment on follicular development were assessed by morphometric analyses by measuring follicle diameter, thecal thickness, and a proliferation index for granulosa cells. Follicular atresia was detected and quantified using the terminal deoxynucleotidyltransferase-UTP nick end labeling method. Effects on gene expression of VEGF and its receptors, Flt and KDR, were studied by *in situ* hybridization. VEGF Trap R1R2 treatment resulted in a significant decrease in thecal proliferation and endothelial cell area, demonstrating the suppression of thecal angiogenesis. The absence of a normal thecal vasculature was associated with a significantly reduced thecal thickness. Antral follicular development was severely compromised, as indicated by decreased granulosa cell proliferation, decreased follicular diameter, and lack of development of ovulatory follicles. Furthermore, the rate of atresia was significantly increased. VEGF expression in granulosa and thecal cells increased after treatment, whereas Flt and KDR expressions in thecal endothelial cells were markedly decreased. These results show that VEGF Trap treatment is associated with the suppression of follicular angiogenesis, which results in the inhibition of antral follicular development and ovulation. (*Endocrinology* 143: 2797–2807, 2002)**

THE OVARY IS distinctive in being a site of active angiogenesis in the adult. Angiogenesis takes place in the developing follicle before ovulation and in the corpus luteum formed postovulation (1–4). It is now well established that active cyclical angiogenesis plays a key role in normal luteal function (1, 4). However, its contribution to normal follicular growth and function has not been addressed experimentally. Thus, little is known about the direct relevance of the thecal vasculature for follicular growth, development, and atresia. Although small preantral follicles are avascular, angiogenesis is initiated during early follicular development and continues throughout follicular growth. The vascular sheath that develops during follicular maturation in the thecal compartment expands with ongoing folliculogenesis (3). The thecal capillaries do not penetrate the membrana propria, so the granulosa compartment remains avascular until breakdown of the basement membrane at ovulation.

The vasculature of the follicle is thought to be necessary for the delivery of hormones, hormone precursors, oxygen, and nutrients. It has been suggested that the preferential delivery of gonadotropins via a more highly developed vascular system in individual follicles plays an instrumental role in the selection and growth of the dominant follicle (5). The relationship between changes in angiogenesis and onset of atresia is uncertain due to difficulties in determining the temporal relationship between these processes, but decreased vascularity in atretic follicles has been reported in a number of species (5–7), including the marmoset (3).

With regard to the molecular mechanisms controlling follicular angiogenesis, the presence of the vascular endothelial growth factor (VEGF), a principal angiogenic factor, has been described in the ovarian follicle (8, 9). More recently, we have demonstrated by direct inhibition of VEGF *in vivo* in the primate that VEGF is a major regulator of follicular angiogenesis (3). Inhibition of VEGF was followed by a severe restriction of thecal angiogenesis in the developing follicle. To investigate the importance of the thecal vasculature for follicular maturation, the approach of suppressing thecal angiogenesis by *in vivo* inhibition of VEGF was used in the current study. A new compound, VEGF Trap R1R2, comprising the extracellular domain of the two VEGF receptors, VEGF-R1 (Flt) (fms-like tyrosine kinase) and VEGF-R2 (KDR) (kinase insert domain-containing receptor), was administered to marmoset monkeys throughout the follicular phase. The efficacy of VEGF Trap R1R2 to suppress thecal angiogenesis was tested using bromodeoxyuridine (BrdU) immunocytochemistry as a proliferation marker, CD31 as a specific endothelial cell marker and dual staining to dis-

Abbreviations: BrdU, Bromodeoxyuridine; Flt, fms-like tyrosine kinase; KDR, kinase insert domain-containing receptor; NBT, nitro blue tetrazolium; TBS, Tris-buffered saline; TUNEL, terminal deoxynucleotidyltransferase-UTP nick end labeling; VEGF, vascular endothelial growth factor.



CELLTRION EXHIBIT - 1016
Celltrion, Inc. v. Regeneron Pharmaceuticals, Inc.

tinguish between proliferating endothelial and nonendothelial cells. The influence on follicular development was assessed by morphological and morphometric image analyses as well as quantification of granulosa cell proliferation. As granulosa cells of the follicle die of apoptosis during the process of atresia (10), the terminal deoxynucleotidyltransferase-UTP nick end labeling (TUNEL) method was used to detect apoptotic granulosa cells for definite classification and quantification of atretic follicles. The effects of inhibition of VEGF on the expression of VEGF and its receptors Flt and KDR was investigated using *in situ* hybridization.

## Materials and Methods

### *VEGF Trap R1R2*

The VEGF Trap R1R2 used in these experiments is a recombinant chimeric protein comprising portions of the extracellular, ligand binding domains of the human VEGF receptors Flt-1 (VEGF-R1, Ig domain 2) and KDR (VEGF-R2, Ig domain 3) expressed in sequence with the Fc portion of human IgG (Fig. 1). The presence of the Fc domain results in homodimerization of the recombinant protein, thereby creating a high affinity (KD1–5pM) VEGF Trap.[1] The VEGF trap was expressed in CHO cells and was purified by protein A affinity chromatography followed by size-exclusion chromatography. The specificity of VEGF binding and the affinity to VEGF of VEGF Trap R1R2 were determined by Biacore (Uppsala, Sweden).

### *Animals*

Adult female common marmoset monkeys (*Callithrix jacchus*) with a body weight of approximately 350 g and regular ovulatory cycles (28-d cycle length) with ovulation on d 8 were housed together with a younger sister or prepubertal female as described previously (11). Blood samples were collected three times per week by femoral venipuncture without anesthesia, and plasma was subjected to progesterone assay as described previously (4).

### *Treatment*

Experiments were carried out in accordance with the Animals (Scientific Procedures) Act, 1986, and were approved by the local ethical review process committee. To synchronize timing of ovulation during the pretreatment cycle, marmosets were given $PGF_{2\alpha}$ in the mid to late luteal phase to induce luteolysis. In the late luteal phase of the subsequent cycle, four marmosets were treated with VEGF trap at a dose of 25 mg/kg, injected sc on d 0, 2, 4, 6, and 8 of the follicular phase. Ovaries were collected 2 d later on d 10 of the cycle. Eleven control marmosets were studied (four on d 1–2, three on d 7–8, and four at d 11 of the cycle). Control animals were treated with vehicle containing 5 mM phosphate, 5 mM citrate, 100 mM sodium chloride, 0.1% (wt/vol) Tween 20, and 20% (wt/vol) sucrose. All animals were injected iv with 20 mg BrdU (Roche Molecular Biochemicals, Essex, UK) in saline 1 h before being sedated using 100 $\mu$l ketamine hydrochloride (Parke-Davis Veterinary, Pontypool, UK) and killed with an iv injection of 400 $\mu$l Euthetal (sodium pentobarbitone, Rhone Merieux, Harlow, UK). After cardiac exsanguination via a heparinized syringe, ovaries were removed immediately and fixed in 4% neutral buffered formalin. After 24 h, the ovaries were put into 70% ethanol, dehydrated, and embedded in paraffin according to standard procedures.

### *Hematoxylin-eosin staining*

The embedded ovaries were serially sectioned, and tissue sections (5 $\mu$m) were placed onto BDH SuperFrost slides (BDH, Merck & Co., Inc., Poole, UK). For morphological and morphometric analyses every 20 of a total of 200 sections/ovary were used. Sections in between were subjected to immunocytochemistry, *in situ* hybridization, and TUNEL. Tissue sections were dewaxed in xylene, rehydrated in descending concentrations of ethanol, washed in distilled water, and stained with hematoxylin (Richard-Allan, Richland, MI) for 5 min, followed by a wash in water and acetic alcohol before staining with eosin (Richard-Allan) for 20 sec. After dehydrating in ascending concentrations of ethanol and xylene, sections were mounted.

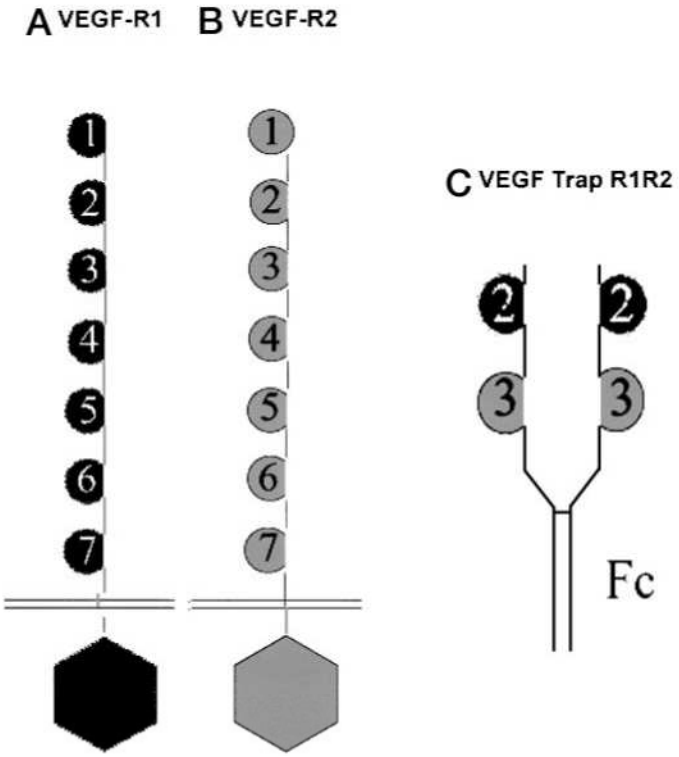


FIG. 1. Structure of VEGF receptors and the VEGF Trap. VEGF-R1 (A) and VEGF-R2 (B) both contain seven extracellular domains, which differ between the two receptors. These extracellular domains are responsible for VEGF binding. The soluble VEGF Trap R1R2 (C) was created by fusion of domain 2 of VEGF-R1 and domain 3 of VEGF-R2 with the FC portion of IgG.

### *Immunocytochemistry*

The effects of the treatment on the establishment of the thecal vascular network were studied by 1) quantifying the number of proliferating cells stained for BrdU, 2) identifying endothelial cells using CD31 staining, and 3) distinguishing proliferating endothelial from nonendothelial cells by colocalization of BrdU and CD31.

For BrdU and CD31 immunostaining, antigen retrieval was performed by pressure cooking (Tefal Clypso pressure cooker, Tefal, Essex, UK) sections in 0.01 M citrate buffer, pH 6, for 6 min at high pressure setting 2. Slides were then left for 20 min in hot buffer and washed in TBS (0.05 mol/liter Tris and 9 g/liter NaCl). To reduce nonspecific binding sections were blocked in normal rabbit serum (1:5 diluted in TBS containing 5% BSA) for 30 min. Primary antibodies CD31 (mouse antihuman CD31, DAKO Corp., Copenhagen, Denmark) or BrdU (mouse anti-BrdU, Roche Molecular Biochemicals) were diluted 1:20 or 1:30 in TBS, respectively. Incubation was carried out overnight at 4 C. Slides were washed three times in TBS. Incubation with the secondary antibody, rabbit antimouse Ig (1:60 diluted in NRS:TBS; DAKO Corp.), was performed for 40 min at room temperature, followed after two washes in TBS by incubation of the alcaline phosphatase-antialcaline phospholase (APAAP) complex (1:100 dilution in TBS, DAKO Corp.) for 40 min at room temperature. Visualization was performed using 500 $\mu$l/slide nitro blue tetrazolium (NBT) solution containing 45 $\mu$l NBT substrate (Roche Molecular Biochemicals), 10 ml NBT buffer, 35 $\mu$l 5-bromo-3-chloro-3-indolyl-phosphate, and 10 $\mu$l levamisole. Sections for BrdU

[1] The detailed molecular structure and how it was created are described in the patent REG 710-A-PCT, VEGF Trap Application published December 2000, Publication WO 00/75319 A1.

Downloaded from https://academic.oup.com/endo/article/143/7/2797/2989719 by Associated Press user on 06 January 2023

were counterstained with hematoxylin, whereas sections for CD31 were not counterstained, so that quantitative image analysis could be performed. For dual labeling, slides were incubated first with CD31 and visualization with Fast Red [Sigma, Poole, UK; 1 mg Fast Red in 1 ml Fast Red buffer (20 mg naphtol AS-MX phosphate, 2 ml dimethyl formamide, and 98 ml 0.1 M Tris, pH 8.2)]. After staining for CD31, incubation with BrdU was performed. BrdU-stained cells were visualized with NBT as described above.

### *In situ hybridization*

*In situ* hybridization was performed as described previously (4, 12). As the marmoset shows 97–98% homology of the known gene sequence with human genome, cRNA probes for human VEGF, Flt, and KDR were used. Sense and antisense probes were prepared using an RNA transcription kit (Ambion, Inc. Austin, TX) and were labeled with [$^{35}$S]-uridine 5[prime]-triphosphate (NEN Life Science Products, Boston, MA). Deparaffinized sections were treated with 0.1 N HCl and then digested in proteinase K (5 $\mu$g/ml; Sigma) for 30 min at 37 C. After prehybridization for 2 h at 55 C subsequent hybridization was performed in a moist chamber overnight. High stringency posthybridization washings and ribonuclease treatment were used to remove excess probe. Slides were then dehydrated, dried, and dipped in Ilford G5 liquid emulsion (H. A. West, Edinburgh, UK). Exposure times for VEGF, Flt, and KDR were 4, 7, and 7 wk, respectively. Slides were subsequently developed (D19 developer, Kodak, Rochester, NY) and fixed (GBS, Kodak). All slides were counterstained with hematoxylin (Richard-Allan, Richland, MI), dehydrated, and mounted.

### *In situ TUNEL*

It is known that during atresia granulosa cells undergo programmed cell death, apoptosis. Hence, the TUNEL method for detection of apoptotic cells was used to identify atretic follicles. Dewaxed and rehydrated slides were incubated for 6 min in 20 $\mu$g/ml proteinase K (Sigma) at room temperature and blocked with normal sheep serum (1:5 dilution). Slides were washed three times in TBS. For 3′-end labeling the TdT Kit (Roche Molecular Biochemicals) was used. 3′-OH ends of DNA fragments were labeled with 1 nM digoxigenin-11-deoxy-UTP (Roche Molecular Biochemicals) for 1.5 h at 37 C by 1 IU/$\mu$l TdT (Roche Molecular Biochemicals) in 50 $\mu$l buffer [30 mM Tris-HCl (pH 7.2), 140 mM sodium cacodylate, and 1.5 mM $CoCl_2$; Roche Molecular Biochemicals). Negative control slides had the TdT replaced by the equivalent amount of buffer. Three rinses of the slides with TBS were followed by incubation with alkaline phosphatase-conjugated sheep anti-digoxigenin antibodies (1:100 dilution; Roche Molecular Biochemicals) in TBS for 90 min at room temperature. The labeling was visualized with NBT as described above. After air-drying, slides were put into xylene and mounted.

### *Analysis of data*

Quantitative analysis was performed using an image analysis system linked to an Olympus Corp. camera, and the data were processed using Image-Pro Plus version 3.0 for Windows (Microsoft Corp.).

### *Morphological characterization of ovarian follicles*

Stages of follicular development were defined as follows: primary follicles (containing only one granulosa cell layer), early secondary follicles (two to four granulosa cell layers, no antrum), late secondary follicles (more than four granulosa cell layers, no antrum), tertiary follicles (follicles containing an antrum), and ovulatory follicles (large antral follicles, >2 mm). Follicles were classified as healthy if they contained a normal-shaped oocyte surrounded by granulosa cells that were regularly apposed on an intact basement membrane with normal appearance of granulosa cell nuclei without signs of pycnosis. Follicles not fulfilling these criteria were classified as unsuitable for analyses. Only follicles with a visible oocyte containing a nucleus were considered to ensure proper follicular classification.

### *Morphometric analyses*

Serial sections of both ovaries of each animal stained for hematoxylin-eosin were subjected to morphometric analyses (10 sections at a distance of 100 $\mu$m/ovary from each other). A total of 31 primary, 523 secondary, and 181 tertiary follicles were analyzed in controls, and 29 primary, 327 secondary, and 77 tertiary follicles were analyzed in treated animals. The image analysis system was set up to measure two diameters of the follicles in a right angle. From these diameters the mean follicular diameter was calculated. Furthermore, the thecal compartment was outlined, and the mean thecal thickness was measured.

### *Quantification of immunocytochemistry, in situ hybridization, and 3′-end labeling*

From our previous study (3) it was known that angiogenesis is initiated in follicles containing more than four granulosa cell layers. Thus, in this study only follicles with four or more granulosa cell layers were analyzed. In all follicles the whole cross-sections were analyzed. Captured images were thresholded, and the thecal and granulosa cell compartments were outlined and analyzed separately.

### *BrdU labeling*

Four sections per ovary were analyzed under ×200 magnification. The image analysis system was set up to measure the number of dark-stained nuclei (BrdU positive), and the number of dark- and light-stained nuclei (total number of cells) in the outlined compartment of interest. A proliferation index (*i.e.* BrdU-positive cells expressed as a percentage of the total number of cells) was calculated in the thecal and granulosa compartments for each follicle. The proliferation index was expressed as a mean value for the number of follicles assessed within each follicular stage and per animal.

The automated image analysis of BrdU in the granulosa of secondary follicles failed to reliably distinguish between single cells because granulosa cells have only a small cytoplasmic volume, so that the nuclei of different cells are in close vicinity. Thus, the granulosa cell proliferation index in these follicles was obtained by manual counting using an eyepiece with a grid.

### *CD31 labeling*

The endothelial cell area (*i.e.* CD31-positive cells) was measured at ×200 magnification in four sections of each ovary. The captured gray scale image was thresholded and converted to a binary image. The whole area of the thecal compartment and the CD31-positive area within the compartment was measured. The CD31-positive area was then calculated per unit area of the thecal compartment and expressed as a mean value for the number of follicles assessed within each follicular stage and per animal.

### *3′-End labeling*

Four sections per animal were analyzed. Follicles were classified as atretic if more than approximately 20% of the granulosa cells were apoptotic. The number of atretic and healthy late secondary and antral follicles were counted manually, and an index for atresia (atretic follicles expressed as a percentage of total number of follicles) was calculated.

### *Statistical analysis*

Data obtained for different cycle and follicular stages were tested for significant differences using ANOVA, followed by Duncan's multiple range test. Effects of the treatment compared with late follicular controls were determined using a two-tailed, unpaired $t$ test. Differences were considered to be significant at $P < 0.05$. The tests were performed using SPSS version 6.1 for Macintosh (SPSS, Inc., Chicago, IL). All values are given as the mean ± SEM.

## Results

### *Efficacy of the treatment to suppress thecal angiogenesis*

Dual staining for BrdU and CD31 (Fig. 2A) showed the established microvasulature in controls. Besides numerous single-stained cells for BrdU, some BrdU-positive cells were also associated with CD31 staining, indicating proliferating

Downloaded from https://academic.oup.com/endo/article/143/7/2797/2989719 by Associated Press user on 06 January 2023

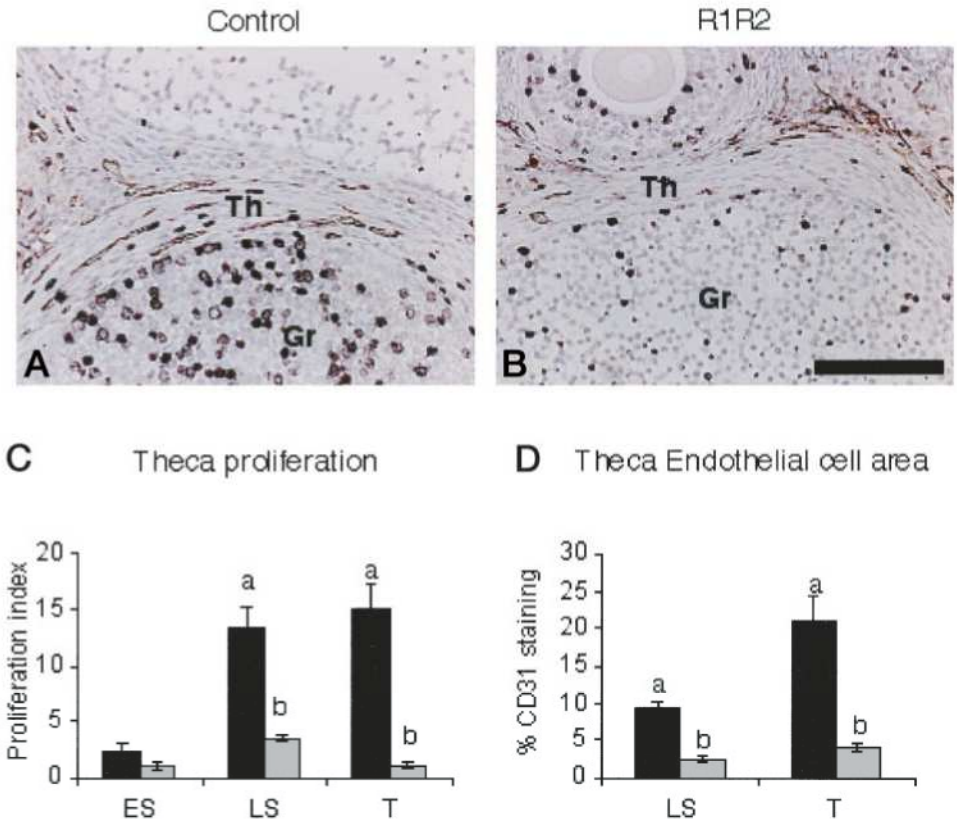


FIG. 2. Dual staining for CD31 (*red* staining) and BrdU (*black* nuclei) in a follicle of a control (A) and an R1R2-treated animal (B). Note the reduction of proliferating cells (single and dual stained) and endothelial staining in the theca (Th) after treatment. Quantification of thecal proliferation (C) revealed a significant decrease in late secondary (LS) and tertiary (T) follicles. In these follicle stages the endothelial cell area (D) was also significantly reduced, demonstrating the suppression of thecal angiogenesis after treatment. Different letters indicate significant differences. ■, controls; ▨, R1R2 treated. ES, Early secondary follicle. *Bar*, 100 $\mu$m.

endothelial cells. After R1R2 treatment (Fig. 2B), very few proliferating cells were visible, and thecal CD31 staining was markedly reduced. These observations were confirmed by quantitative analyses (Fig. 2, C and D). The thecal proliferation index in late secondary follicles was 13.6 ± 2.8% in early follicular controls, 13.2 ± 1.8% in late follicular controls, and 13.4 ± 1.4% in early luteal controls. After treatment, a 79% reduction ($P < 0.05$) of thecal proliferation was found in late secondary follicles (3.4 ± 0.6%). The thecal proliferation index of tertiary follicles was 10.6 ± 0.4% in early follicular controls, 15.1 ± 2.1% in late follicular controls, and 16.2 ± 2.0% in early luteal controls. After R1R2 treatment, a major 92% reduction ($P < 0.001$) in thecal proliferation in tertiary follicles (1.1 ± 0.2%) was observed.

The endothelial cell areas measured in secondary or tertiary follicles of control animals were comparable (in secondary follicles, 0.09 ± 0.01 $\mu m^2$/unit area during the early follicular phase, 0.09 ± 0.008 $\mu m^2$/unit area during the late follicular phase, and 0.09 ± 0.008 $\mu m^2$/unit area during the early luteal phase; in tertiary follicles, 0.2 ± 0.01 $\mu m^2$/unit area during the early follicular phase, 0.2 ± 0.03 $\mu m^2$/unit area during the late follicular phase, and 0.18 ± 0.02 $\mu m^2$/unit area during the early luteal phase). After R1R2 treatment a significant reduction of the endothelial cell area of 72% was found in secondary follicles (0.025 ± 0.005 $\mu m^2$/unit area) and 80% in tertiary follicles (0.04 ± 0.007 $\mu m^2$/unit area). In summary, it was evident that the treatment efficiently suppressed thecal angiogenesis in secondary and tertiary follicles.

### *Effects of R1R2 treatment on thecal development*

Thecal development is initiated during early follicular growth when a follicle contains more than two granulosa cell layers. The fully differentiated theca is shown in Fig. 3A. Thecal cells have an elongated flat appearance surrounding the granulosa compartment in several layers. Fibrocytes are dispersed within these layers as the microvasculature is established. After R1R2 treatment (Fig. 3B), thecal cells appeared swollen, contained enlarged nuclei, and had lost their elongate shape. Furthermore, the theca lacks a microvasculature. In contrast, the occurrence of fibrocytes appeared unaffected.

By measuring thecal thickness and plotting against the follicular diameter (Fig. 3C), a significant linear correlation was found for secondary follicles in controls ($r = 0.9$; $P < 0.001$) and treated animals ($r = 0.86$; $P < 0.001$). However, after R1R2 treatment the slope of the curve was reduced, indicating that at a given follicle diameter the theca is thinner than that in controls. Comparison of the mean thecal thickness in these follicles confirmed a significant reduction ($P < 0.05$) in thecal thickness after treatment. No correlation between thecal thickness and follicle diameter was observed in tertiary follicles.

### *Effects of R1R2 treatment on the expression of VEGF and its receptors KDR and Flt*

In controls, VEGF mRNA was expressed in the granulosa and to a lesser extent in the thecal compartment in secondary and tertiary follicles (Fig. 4A). An increase in

Downloaded from https://academic.oup.com/endo/article/143/7/2797/2989719 by Associated Press user on 06 January 2023

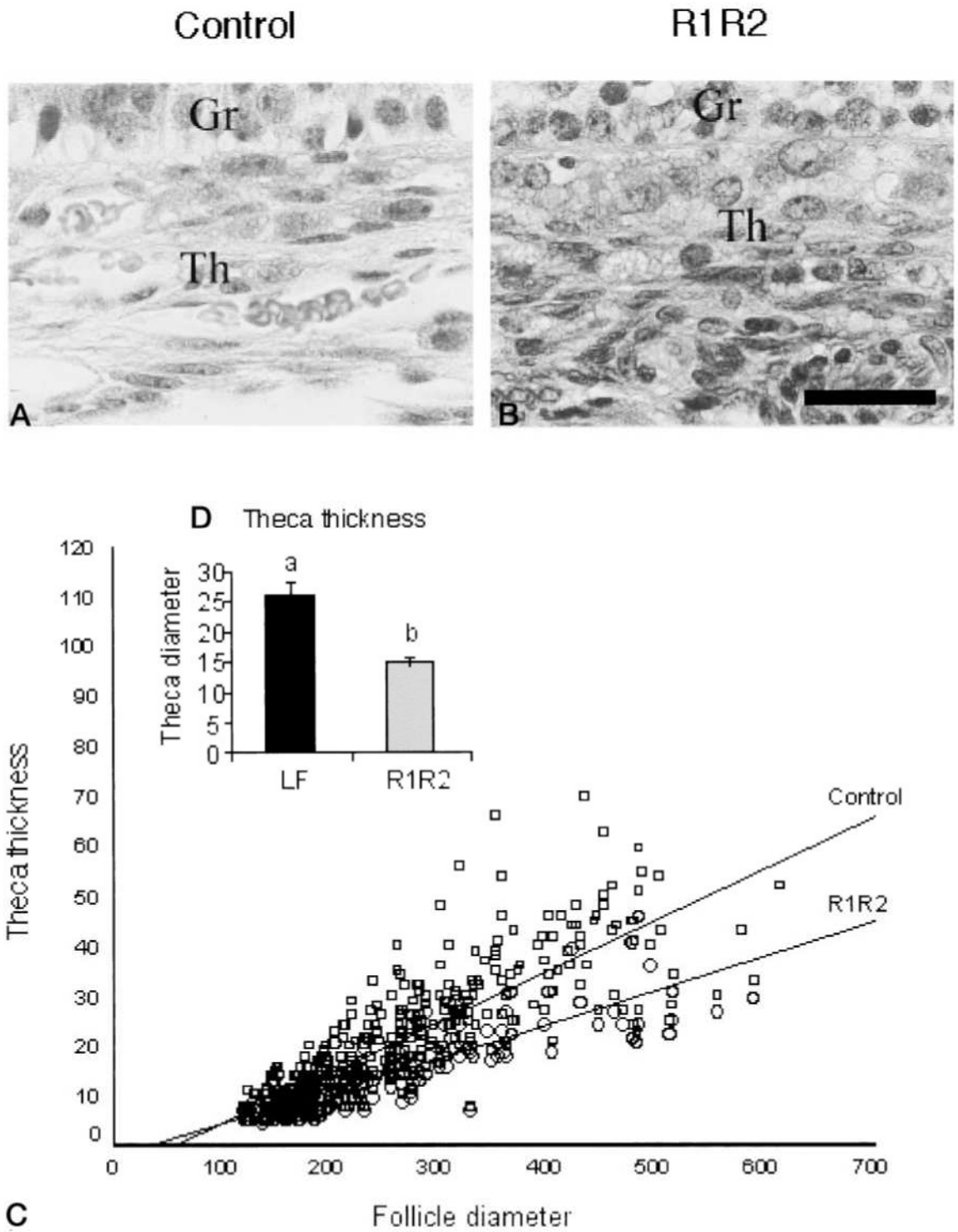


FIG. 3. Effects of the inhibition of thecal angiogenesis on thecal development. A, A hematoxylin- and eosin-stained section of the theca (Th) of a control. Thecal cells have an elongated, flattened shape. Capillaries pass through the thecal compartment. B, Thecal cells after R1R2 treatment appear swollen with enlarged nuclei. Note the lack of the thecal capillaries (*bar*, 100 $\mu$m). Measuring the thecal thickness and plotting it against the follicle diameter (C), a significant linear correlation for both in controls and after R1R2 treatment was found. However, the curve for the R1R2 treatment exhibited a lower slope, indicating that the theca after treatment is thinner. This was confirmed by comparison of the mean thecal diameters (D). *Different letters* indicate significant differences. LF, Late follicular control.

Downloaded from https://academic.oup.com/endo/article/143/7/2797/2989719 by Associated Press user on 06 January 2023

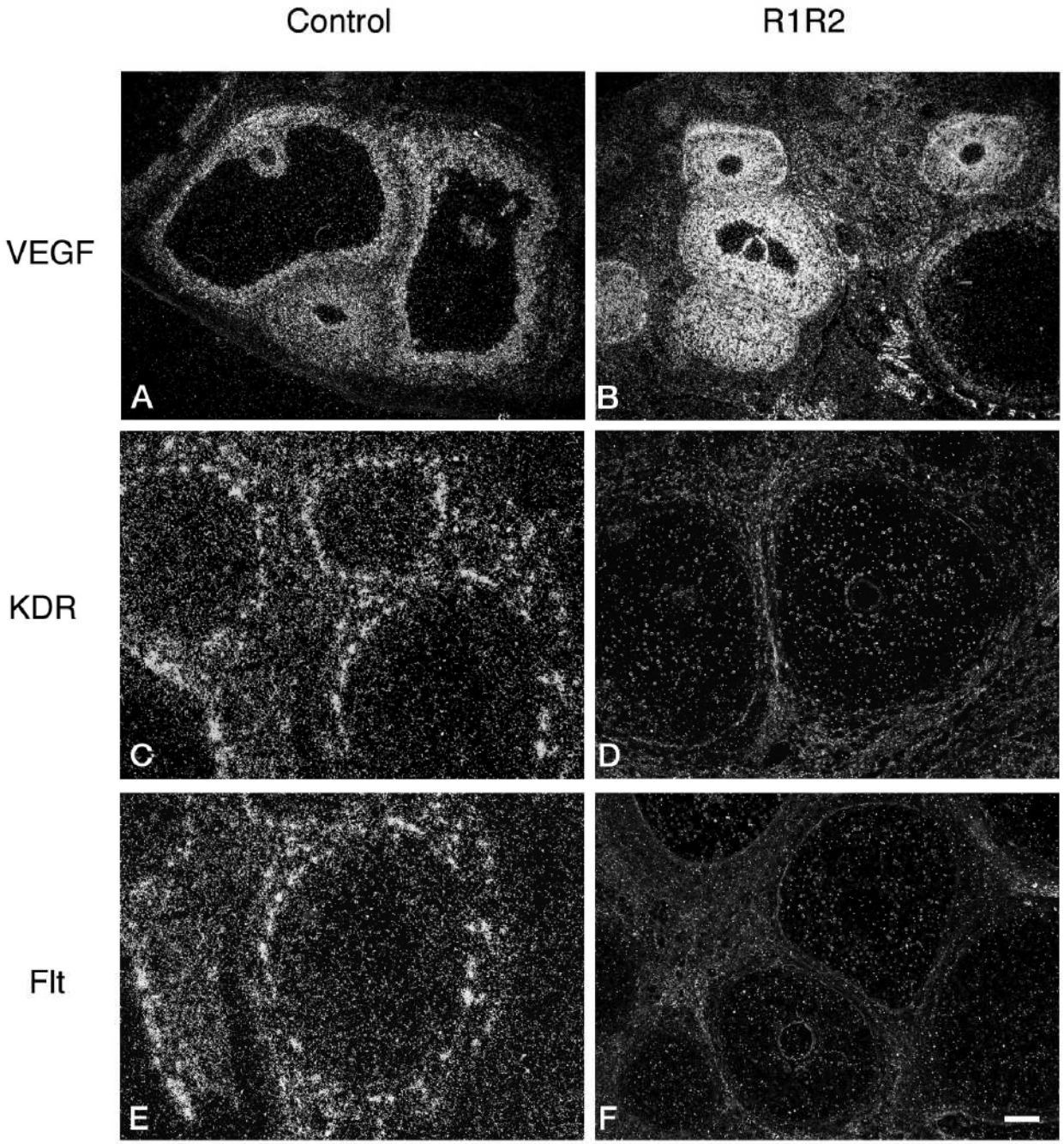


FIG. 4. Effects of the treatment on the gene expression of VEGF (A and B), KDR (C and D), and Flt (E and F). After treatment, VEGF was expressed in increasing amounts in the thecal and granulosa cell compartments of secondary and tertiary follicles. KDR (B) and Flt (E) mRNA was localized in thecal endothelial cells, and after treatment a complete down-regulation was notable (D and F). *Bar*, 50 $\mu$m.

VEGF expression in the granulosa was observed in the preovulatory follicles. After R1R2 treatment (Fig. 4B) VEGF mRNA expression was markedly increased in the granulosa of secondary and tertiary follicles. Expression in the theca was also increased, especially in secondary follicles, such that the expression in the theca appeared to be higher than that in the granulosa. The KDR receptor mRNA (Fig. 4C) and Flt receptor mRNA (Fig. 4E) are both expressed in the endothelium of the thecal vasculature of both secondary and tertiary follicles. A complete down-regulation of both receptors (Fig. 4, D and F) was found after R1R2 treatment. This decrease was attributable not only to the dearth of thecal endothelial cells after treatment, but also to a reduction in expression in the remaining cells.

*Secondary effects of the treatment on follicular development*

By gross inspection, it appeared that after R1R2 treatment ovaries were smaller than controls. No signs of an ovulatory

Downloaded from https://academic.oup.com/endo/article/143/7/2797/2989719 by Associated Press user on 06 January 2023

follicle or an ovulation stigma were found, which were observed in late follicular or early luteal controls. A significant decrease in ovarian weight (37 ± 6.9 mg) after treatment was measured compared with early follicular (113 ± 12 mg), late follicular (70 ± 13 mg), and early luteal (127 ± 35 mg) controls.

In a cross-section through a typical control ovary of the early follicular phase (d 1–2; Fig. 5A) the regressing luteal tissue of the previous cycle was visible, occupying the majority of the organ. Numerous healthy and atretic small and medium sized antral follicles were also present. In the late follicular phase ovary (d 7–8; Fig. 5B) the predominant feature was the developed preovulatory follicles (two or three per animal). Besides these, a number of smaller antral follicles are located within the cortex. After ovulation (d 10–11; Fig. 5C), the early corpus luteum dominates, occupying two thirds of the ovary. Medium and large antral follicles, a number of them either luteinized or atretic, are present within the cortex. After R1R2 treatment, the most striking observation is the absence of medium and large antral follicles (Fig. 5D). A small proportion of regressed luteal tissue from the previous cycle was visible, but fresh, healthy corpora lutea were absent.

Depending on the stage of follicular development, granulosa cell proliferation was also effected by the treatment. In secondary follicles of controls (Fig. 6A) numerous granulosa cells were BrdU positive, indicating active cell proliferation. After R1R2 treatment no differences were apparent (Fig. 6B). In tertiary follicles of controls (Fig. 6C) a large number of granulosa cells are also proliferating, whereas after treatment (Fig. 6D) the number of proliferating granulosa cells markedly decreased. Quantification (Fig. 6E) confirmed these observations, showing a nonsignificant decrease in secondary follicles and a significant reduction in the proliferation index after R1R2 treatment in tertiary follicles.

The results of granulosa cell proliferation are consistent with morphometric analysis of follicular diameter. There was no difference in follicle diameter of early follicular stages (primary and early secondary follicles). Also no differences were observed for late secondary follicles between early follicular phase (167 ± 9.1 $\mu$m), late follicular phase (174 ± 8.1 $\mu$m), early luteal phase (161 ± 5.2 $\mu$m), and after R1R2 treatment (171 ± 5 $\mu$m). However, major differences were detectable in tertiary follicles. Frequency measurements revealed that in controls, the peak frequency of tertiary follicles was 950 $\mu$m (Fig. 7A). A smaller number of large antral follicles (>1300 $\mu$m) and ovulatory follicles (~2500 $\mu$m) were also present. In comparison, in R1R2-treated animals (Fig. 7B) the peak frequency was reduced (750 $\mu$m). Most striking was the absence of follicles over 1000 $\mu$m. Comparison of the mean follicular diameter of tertiary follicles (Fig. 7C) showed a significantly decreased diameter in follicles after R1R2 treatment (722 ± 13 $\mu$m) compared with controls (973 ± 31 $\mu$m).

The TUNEL method to detect apoptosis in follicles to classify them definitely as atretic (*i.e.* the percentage of apoptotic follicles of the total number of follicles) showed that atresia

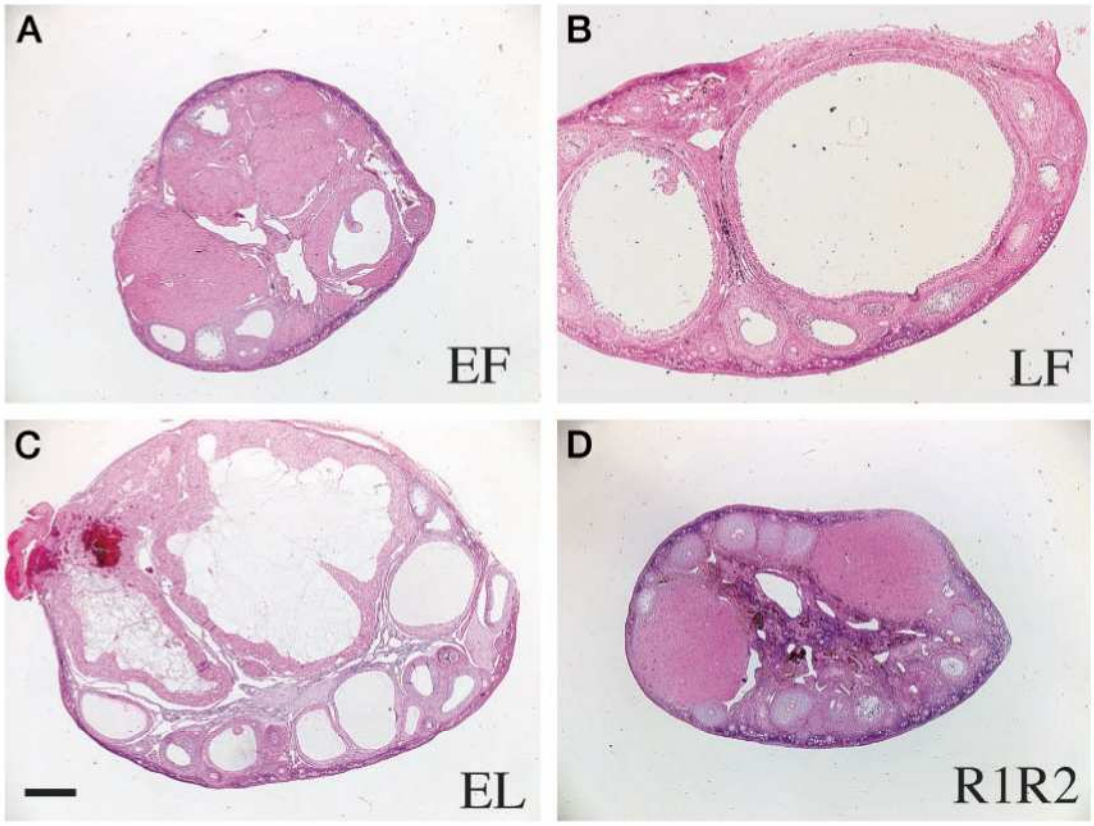


FIG. 5. Effects of the inhibition of thecal angiogenesis on follicular development. Hematoxylin- and eosin-stained sections of the early follicular phase (A), late follicular phase (B), and early luteal phase (C) and after R1R2 treatment (D) are shown. Note the lack of large antral follicles after treatment compared with all other stages. *Bar*, 200 $\mu$m.

Downloaded from https://academic.oup.com/endo/article/143/7/2797/2989719 by Associated Press user on 06 January 2023

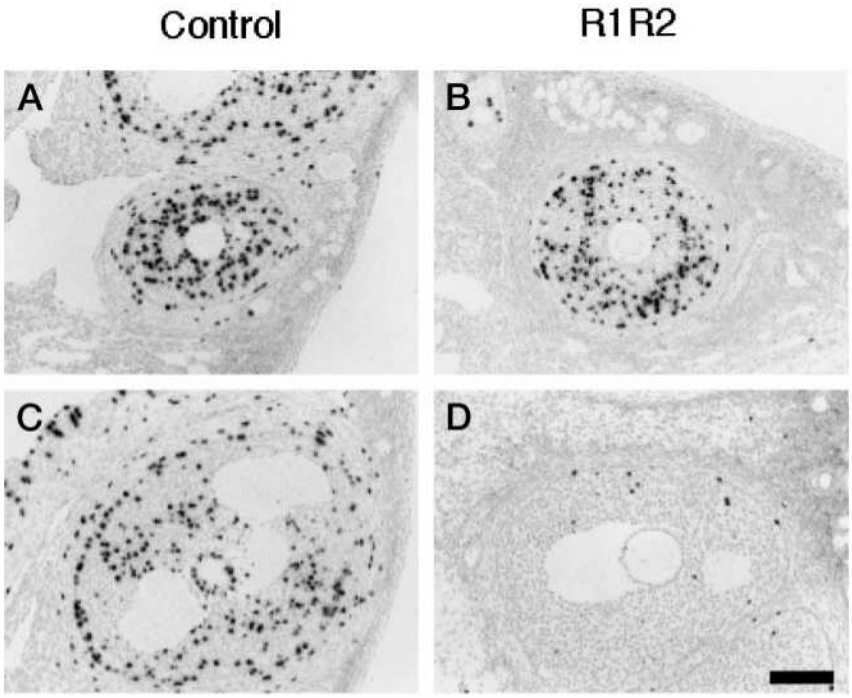


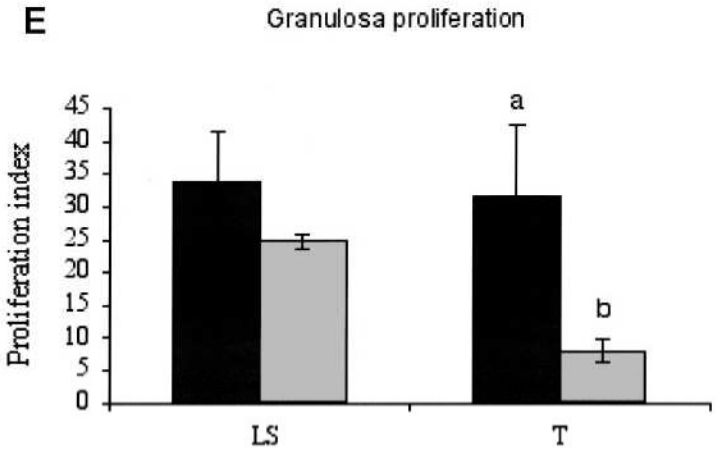


FIG. 6. Effects of the treatment on granulosa cell proliferation as indicated by BrdU immunocytochemistry. A, A late secondary follicle (LS) of a control ovary; B, a comparable follicle after treatment. No obvious differences in BrdU staining (*black* nuclei) are visible. C and D, A tertiary follicle of a control and R1R2-treated ovary is shown, respectively. Note the decline in granulosa cell proliferation after the treatment (*bar*, 100 $\mu$m). Quantitative analyses (E) confirmed the observation of decreased granulosa cell proliferation in antral follicles after treatment (▨) compared with controls (■).

was rarely detectable in follicles up to the late secondary stage, and no quantitative difference in atresia was found between controls and R1R2-treated animals. In tertiary follicles, atresia did not vary between the normal cycle phases, being 37 ± 1.6% during the early follicular phase, 35 ± 6.8% during the late follicular phase, and 41 ± 4.3% during the early luteal phase. However, after R1R2 treatment, a significant doubling (78 ± 4%) in the atretic rate was found compared with all controls (Fig. 7D).

## Discussion

This study has established the importance of the thecal vasculature for follicular development by inhibiting VEGF using a novel antagonist, VEGF Trap R1R2, throughout the follicular phase of the cycle. Treatment resulted in suppression of thecal angiogenesis in secondary and tertiary follicles. As a secondary effect, the development of the theca was impaired. VEGF expression was increased, whereas its receptor gene expression was decreased. Most important, this is the first report demonstrating that suppression of follicular angiogenesis is associated with inhibition of antral follicular development, resulting in the prevention of ovulation.

In a previous study (3) using VEGF $Trap_{A40}$, an antagonist comprising only the extracellular domain of the Flt-1 receptor, thecal proliferation was also reduced in secondary and tertiary follicles, but to a lesser extent, and the endothelial cell area was decreased only in tertiary follicles. VEGF Trap R1R2 may be more efficient in inhibiting VEGF, because it contains an additional domain of the second VEGF receptor KDR; fusion of both receptors significantly improved the pharmacokinetic profile without losing affinity. However, full dose-response studies would be necessary to determine whether VEGF Trap R1R2 does inhibit VEGF more effectively. The more profound effects observed herein are most likely the

Downloaded from https://academic.oup.com/endo/article/143/7/2797/2989719 by Associated Press user on 06 January 2023

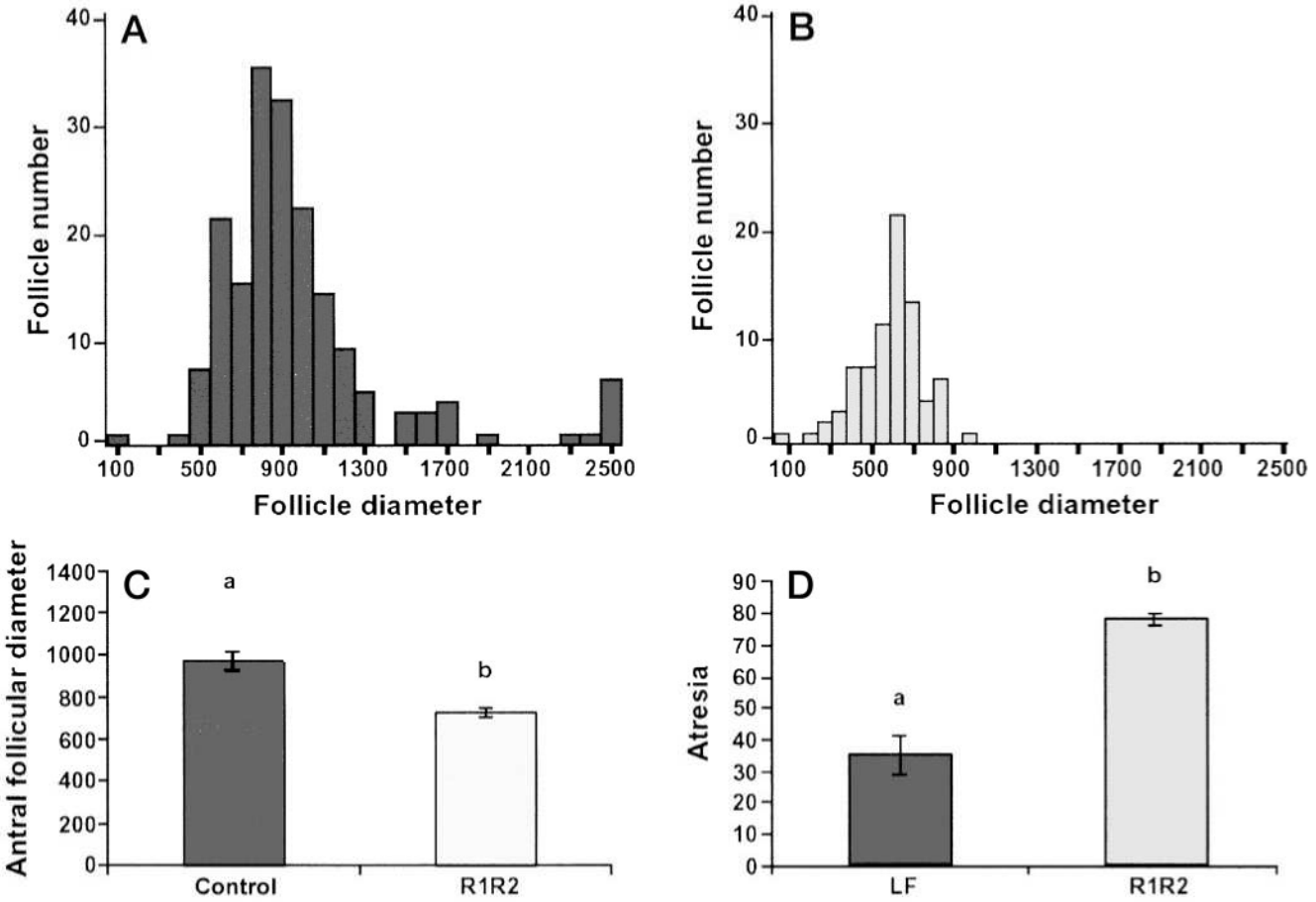


FIG. 7. Effects on antral follicular development. Frequency measurements of follicles of controls (A) and after R1R2 (B). Mean frequency of controls is 975 $\mu$m; after treatment the mean frequency was reduced to 722 $\mu$m. Also note the lack of medium and large antral follicles over 1000 $\mu$m in the ovaries of treated animals. Comparison of the mean diameter (C) confirmed a significant decrease in antral follicular diameters after R1R2 treatment compared with controls. D, Quantification of atretic antral follicles is shown in late follicular controls and after R1R2 treatment. *Different letters* indicate significant differences.

result of the fact that the experiment was designed to inhibit VEGF throughout the 10-d follicular phase, whereas in the former study animals were treated only for 3 d during the luteal phase.

Thecal development precedes follicular angiogenesis (3). In early secondary follicles, proliferation in the theca was detectable before endothelial cell staining, indicating that early thecal development is independent of a microvasculature (3). In the current study a linear correlation between thecal thickness and follicular diameter was found in secondary follicles, indicating that the theca develops during the secondary, preantral stage and is established in antral follicles. By inhibition of VEGF in this study we have established that the thecal development from the late secondary stage onward is dependent on a functional thecal microvasculature. After treatment with VEGF Trap R1R2, proliferation in the theca was dramatically reduced, and thecal thickness was decreased in late secondary and tertiary follicles. As only 25–30% of proliferating cells in the theca are of endothelial cell origin (3), the treatment must have had secondary inhibitory effects on the proliferation of nonendothelial cells, including the hormone-producing thecal cells. This reduction in thecal proliferation together with the absence of thecal capillaries explains why thecal thickness was reduced. The hypertrophic appearance of thecal cells and their enlarged nuclei are probably signs of degeneration, probably as a result of reduced availability of LH, as a consequence of the reduction in vascular development. It is also conceivable that inhibition of VEGF may disrupt pituitary gonadotropin secretion. Because of difficulties in establishing suitable assays for LH and FSH in the marmoset and the relatively infrequent blood sampling, this issue could not be addressed in the present study. Observations in rhesus monkeys, for which assays are available, indicate that anti-VEGF treatment during the follicular phase may result in a small rise in gonadotropins (13).

Although secondary follicular growth, as judged by granulosa cell proliferation, appeared not to be affected by inhibiting VEGF (despite the reduced thecal development), the impairment of thecal microvasculature in tertiary follicles exerted a secondary deleterious effect on antral follicular growth. Follicle diameter is mainly dependent on the size of the granulosa compartment, especially in tertiary follicles. In such follicles, granulosa cell proliferation was severely restricted by treatment; corre-

Downloaded from https://academic.oup.com/endo/article/143/7/2797/2989719 by Associated Press user on 06 January 2023

spondingly the mean follicular diameter of tertiary follicles was significantly reduced, and no follicles over 1000 $\mu$m in diameter were present. This indicates that follicles only grew to a certain size, then stopped, resulting in prevention of the development of an ovulatory follicle. Thus, it seems that the threshold beyond which follicular development (especially the avascular granulosa compartment) is angiogenesis dependent is the early antral stage. The selective suppression of antral follicular development may be due to a reduced availability of gonadotropins, especially FSH, which binds exclusively to the granulosa cells and stimulates cell proliferation (14, 15). FSH binding to granulosa cells is higher in antral than preantral follicles due to differences in FSH receptor density (14). It is believed that FSH is the primary stimulus for antral transition (16), and FSH alone is sufficient to induce antrum formation in human preantral follicles cultured *in vitro* (17). Thus, impairment of the vasculature causing insufficient FSH support would result in suppression of granulosa cell proliferation and antral and especially preovulatory follicular growth. This hypothesis is also in agreement with studies (5) on gonadotropin-binding sites in the rhesus monkey that suggested that increased vascularization of individual follicles results in preferential delivery of gonadotropins, which may play an instrumental role in selective maturation of the preovulatory follicle.

It is difficult to establish the temporal relationship between the onset of atresia and changes in the vasculature. However, a correlation between the impairment of the vasculature and atresia was observed after VEGF R1R2 treatment. FSH has been shown to be a survival factor for granulosa cells (18, 19). Accordingly, reduced availability of FSH due to the lack of a microvasculature after treatment may cause the increase in follicular atresia. Decreased vascularity has been observed in atretic follicles (3, 5–7). It was also shown that the mRNA for VEGF and its receptor was down-regulated in naturally occurring atresia (3). These results suggest that the naturally occurring atretic process could be promoted and maintained by an impairment of thecal angiogenesis.

With regard to the molecular regulation of thecal angiogenesis, it was shown that VEGF was expressed in granulosa and thecal cells of follicles, indicating that VEGF acts in a paracrine manner on the endothelium of the thecal microvasculature. After VEGF inhibition by VEGF Trap R1R2, an increase in gene expression was detectable by *in situ* hybridization. Increased VEGF mRNA levels after VEGF inhibition has also been observed in the corpus luteum (4). It was interesting to note that VEGF mRNA appeared to be preferentially up-regulated in the theca of secondary follicles after treatment. The increase in VEGF expression may be in part driven by a hypoxic response in the follicle, especially in the theca, resulting from the dearth of the vasculature, as it has been shown that hypoxia stimulates VEGF synthesis in other tissues (20–23). In contrast, the VEGF Trap R1R2 treatment had severe inhibitory effects on KDR and Flt receptor mRNA expression in the remaining thecal endothelial cells, indicating that the genes for KDR and Flt were switched off due to the lack of functional VEGF. This implies that VEGF regulates its own receptor expression in follicles as in other tissues (24–26).

In conclusion, this study provides the first clear evidence obtained by *in vivo* experimentation that antral and periovulatory follicular growth, thus ovarian function, is dependent on the establishment of a normal thecal vasculature. VEGF and its receptors appear to be principal regulators of thecal angiogenesis. Defects in thecal vascular development may well be a cause of ovarian dysfunction and infertility. Because cyclic angiogenesis occurs uniquely within the female reproductive tract, the use of antiangiogenic compounds may have important clinical applications (such as for the treatment of polycystic ovary syndrome, ovarian hyperstimulation syndrome, or endometriosis or the regulation of fertility) without having side-effects on other tissues.

## Acknowledgments

We thank Dr. D. S. Charnock-Jones (Department of Obstetrics and Gynecology, University of Cambridge, Cambridge, UK) for the gift of cDNA probes for VEGF, Flt, and KDR; T. Pinner (Medical Research Council of Edinburgh) for graphical support; F. Pitt and I. Swanston for hormone assays; and K. Morris and staff for animal care.

Received November 14, 2001. Accepted March 13, 2002.

Address all correspondence and requests for reprints to: Dr. C. Wulff, Department of Obstetrics and Gynecology, University of Ulm, Prittwitzstrasse 43, 89075 Ulm, Germany. E-mail: christine-wulff@onlinehome.de.

This work was supported in part by a grant from the Deutsche Forschungsgemeinschaft (to C.W.).

## References

1. **Fraser HM, Dickson SE, Lunn SF, Wulff C, Morris K, Carroll VA, Bicknell R** 2000 Suppression of luteal angiogenesis in the primate by neutralization of vascular endothelial growth factor. Endocrinology 141:995–1000
2. **Fraser HM, Wulff C** 2001 Angiogenesis in the primate ovary. Reprod Fertil Dev 13:557–566
3. **Wulff C, Wiegand SJ, Saunders PTK, Scobie GA, Fraser HM** 2001 Angiogenesis during follicular development and its inhibition by Flt-1-Fc (VEGF $Trap_{A40}$) in the primate. Endocrinology 142:3244–3254
4. **Wulff C, Wilson H, Rudge JS, Wiegand SJ, Lunn SF, Fraser HM** 2001 Luteal angiogenesis: prevention or intervention by treatment with vascular endothelial growth factor $Trap_{A40}$. J Clin Endocrinol Metab 86:3377–3386
5. **Zeleznik AJ, Schuler HM, Reichert JRLE** 1981 Gonadotropin-binding sites in the rhesus monkey ovary: role of the vasculature in the selective distribution of human chorionic gonadotropin to the preovulatory follicle. Endocrinology 109:356–362
6. **Moor RM, Seamark RF** 1986 Cell signaling permeability and microvasculatory changes during antral follicle development in mammals. J Dairy Sci 69:927–943
7. **Greenwald GS** 1989 Temporal and topographic changes in DNA synthesis after induced follicular atresia. Biol Reprod 40:175–181
8. **Phillips HS, Hains J, Leung DW, Ferrara N** 1990 Vascular endothelial growth factor is expressed in rat corpus luteum. Endocrinology 127:965–967
9. **Ravindranath N, Little-Ihrig L, Phillips HS, Ferrara N, Zeleznik AJ** 1992 Vascular endothelial growth factor messenger ribonucleic acid expression in the primate ovary. Endocrinology 131:254–260
10. **Kim J-M, Boone DL, Auyeung A, Tsang BK** 1998 Granulosa cell apoptosis induced at the penultimate stage of follicular development is associated with increased levels of Fas and Fas ligand in the rat ovary. Biol Reprod 58:1170–1176
11. **Fraser HM, Dickson SE, Morris KD, Erickson GF, Lunn SF** 1999 The effects of the angiogenesis inhibitor TNP-470 on luteal establishment and function in the primate. Hum Reprod 14:2054–2060
12. **Wulff C, Wilson H, Largue P, Duncan WC, Armstrong DG, Fraser HM** 2000 Angiogenesis in the human corpus luteum: localization and changes in angiopoietins, Tie-2 and vascular endothelial growth factor messenger ribonucleic acid. J Clin Endocrinol Metab 85:4302–4309
13. **Zimmermann RC, Xiao E, Husami N, Sauer MV, Lobo R, Kitajewski J, Ferin M** 2001 Short-term administration of antivascular endothelial growth factor antibody in the late follicular phase delays follicular development in the rhesus monkey. J Clin Endocrinol Metab 86:768–772
14. **Yamoto M, Shima K, Nakano R** 1992 Gonadotropin receptors in human ovarian follicles and corpora lutea throughout the menstrual cycle. Horm Res 37(Suppl 1):5–11
15. **Gougeon A** 1996 Regulation of ovarian follicular development in primates: facts and hypotheses. Endocr Rev 17:121–155

Downloaded from https://academic.oup.com/endo/article/143/7/2797/2989719 by Associated Press user on 06 January 2023

16. **Hirshfield AN** 1991 Development of follicles in the mammalian ovary. Int Rev Cytol 124:43–101
17. **Roy SK, Treacy BJ** 1993 Isolation and long-term culture of human preantral follicles. Fertil Steril 59:783–790
18. **Chun SY, Eisenhauer KM, Minami S, Billig H, Perlas E, Hsueh AJW** 1996 Hormonal regulation of apoptosis in early antral follicles: follicle-stimulating hormone as a major survival factor. Endocrinology 137:1447–1456
19. **Durlinger AL, Kramer P, Karels B, Grootegoed JA, Uilenbroek JT, Themmen AP** 2000 Apoptotic and proliferative changes during induced atresia of preovulatory follicles in the rat. Hum Reprod 15:2504–2511
20. **Rossler J, Breit S, Havers W, Schweigerer L** 1999 Vascular endothelial growth factor expression in human neuroblastoma: up-regulation by hypoxia. Int J Cancer 81:113–117
21. **Popovici RM, Irwin JC, Giaccia AJ, Giudice LC** 1999 Hypoxia and cAMP stimulate vascular endothelial growth factor (VEGF) in human endometrial stromal cells: potential relevance to menstruation and endometrial regeneration. J Clin Endocrinol Metab 84:2245–2248
22. **Ahmed A, Dunk C, Ahmed S, Khaliq A** 2000 Regulation of placental vascular endothelial growth factor (VEGF) and placenta growth factor (PlGF) and soluble Flt-1 by oxygen–a review. Placenta 21(Suppl A):16–24
23. **Neeman M, Abramowitch R, Schiffenbauer YS, Tempel C** 1997 Regulation of angiogenesis by hypoxic stress: from solid tumours to the ovarian follicle. Int J Exp Pathol 78:57–70
24. **Sato Y, Kanno S, Oda N, Abe M, Ito M, Shitara K, Shibuya M** 2000 Properties of two VEGF receptors, Flt-1 and KDR, in signal transduction. Ann NY Acad Sci 902:201–207
25. **Barleon B, Siemeister G, Martiny-Baron G, Weindel K, Herzog C, Marme D** 1997 Vascular endothelial growth factor up-regulates its receptor fms-like tyrosine kinase 1 (FLT-1) and a soluble variant of FLT-1 in human vascular endothelial cells. Cancer Res 57:5421–5425
26. **Shen BQ, Lee DY, Gerber HP, Keyt BA, Ferrara N, Zioncheck TF** 1998 Homologous up-regulation of KDR/Flk-1 receptor expression by vascular endothelial growth factor in vitro. J Biol Chem 237:29979–29985

## STADY III—International Symposium on Signal Transduction in Health and Disease
## 1–4 October, 2002
## Tel Aviv, Israel

For further information, contact Professor Zvi Naor at the following address:

Prof. Zvi Naor
Department of Biochemistry
Tel Aviv University
Ramat Aviv 69978
Israel
Telephone: +972-3-6409032/6417057
Fax: +972-3-6406834
E-mail: naorzvi@post.tau.ac.il or stady2002@unitours.co.il

Downloaded from https://academic.oup.com/endo/article/143/7/2797/2989719 by Associated Press user on 06 January 2023